High Pressure Thermal Conductivity Measurements of Ternary (Methane + Propane + Heptane) Mixtures with a Transient Hot-Wire Apparatus

Dongchan Kim[1] · Saif Z. S. Al Ghafri[1] · Xiaoxian Yang[1] · Sofia K. Mylona[1] · Thomas J. Hughes[1,2] · Luke McElroy[1,3] · Eric F. May[1]

Abstract

The prediction of thermophysical properties for hydrocarbon mixtures at high pressures, and conditions near the phase boundary or critical point is challenging. However, natural gas processing applications have an increasing need for reliable property predictions at such conditions. In this work, thermal conductivity measurements of three ternary mixtures (methane + propane with heptane at concentration up to 15 mol%) were carried out with a transient hot-wire apparatus. Measurements of the three ternary mixtures were conducted over the temperature range from (199.1 to 424.2) K and the pressure range between (10.41 and 31.55) MPa at single phase conditions with a relative combined expanded uncertainty ($k = 2$) between 0.015 and 0.056. The measured values were compared to predictions made with the extended corresponding states (ECS) model and SUPERTRAPP model implemented in the software packages REFPROP 10 and MultiFlash 6.2, respectively. The relative deviations of the measured thermal conductivities from the model predictions were (-5.7 to $+2.4$) % for the ECS model and (-21.1 to -0.6) % for the SUPERTRAPP model. This indicates the latter, older model should not be used to estimate natural gas thermal conductivities, particularly at high pressure conditions, while the ECS model is capable of representing the data within their uncertainty with no parameter tuning required.

✉ Eric F. May
  eric.may@uwa.edu.au

1   Fluid Science & Resources Division, School of Engineering, The University of Western Australia, Perth, Australia

2   Department of Civil Engineering, Monash University, Clayton, VIC 3800, Australia

3   WA School of Mines: Minerals, Energy and Chemical Engineering, Curtin University, Perth, Australia

1 Introduction

The natural gas industry faces challenges associated with reducing the cost and energy consumption of processing equipment. The accurate prediction of thermophysical properties is one means by which this challenge can be addressed, for example by reducing the margins applied during engineering design [1–10]. Thermal conductivity is particularly important to the design of basic process equipment such heat exchangers. In many cases, however, the uncertainty of fluid mixture thermal conductivities predicted using available engineering models exceeds 10 % [11–13], particularly at high pressures and near phase boundaries. This is in part because there are insufficient thermal conductivity data available for mixtures which can be used to tune and/or validate the predictions of different models.

The thermal conductivity for ternary mixtures (methane + propane + heptane) with several different heptane mole fractions (0.05, 0.10 and 0.15) was measured in this work over the temperature range from (199.1 to 424.2) K and the pressure range between (10.41 and 31.55) MPa at single phase conditions and near the phase boundary. The transient hot-wire (THW) technique is a commonly used approach (Perkins et al. [14, 15]; Assael et al. [16, 17]; Wu et al. [18, 19]) that enables an absolute measurement of the thermal conductivity of fluids. The specific descriptions of the technique were summarized by Wakeham et al. [20] and by Assael et al. [21].

In this paper, we present briefly the fundamental theory of the THW technique in Sect. 2.1. The detailed specifications regarding the equipment, gas samples, measurement procedure and measurement uncertainties are summarized in Sects. 2.2 to 2.5, respectively. Validation measurements of pure argon and pure methane, and the measurement results for the target mixtures are presented in Sect. 3, together with comparisons of the data with two models often used for predicting fluid thermal conductivities.

2 Experimental Section

2.1 Measuring Principle

The thermal conductivity measurements were conducted using a THW apparatus developed for use over the temperature range from (193 to 424) K at pressures to 34 MPa. The THW apparatus [11, 12] design was adapted from that of Perkins et al. [22, 23] and is schematically illustrated in Fig. 1. Two wires of different lengths (with electrical resistances R_L and R_S) are installed in the separate arms of a Wheatstone bridge circuit to measure the resistance variation resulting from the heat produced when a transient current is applied from a power source. The variable resistor R_2 installed on the short arm of the bridge is adjusted to balance the bridge voltage ($V_{bridge} \approx 0$) prior to applying the current. According to the theory developed by Kestin and Wakeham [24], when a step change of voltage V_S is applied to the Wheatstone bridge for a short period of time, the temperature
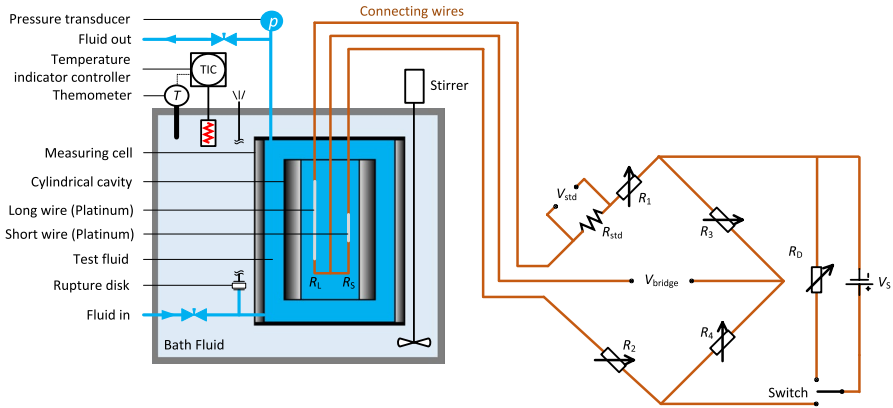
Fig. 1 Schematic diagram of the measuring system

increase in the long wire $\Delta T_{\mathrm{L}}(t)$ at time t and the heat flux per unit length in the long wire q can be calculated, respectively, from measurements of the bridge voltage $V_{\mathrm{bridge}}(t)$ and the voltage across the standard resistor $V_{\mathrm{std}}(t)$. According to the theory developed by Healy et al. [25], corrections should be applied to $\Delta T_{\mathrm{L}}(t)$ to determine the corresponding temperature increase $\Delta T(t)$ for an idealized wire of infinite length. Then, $\Delta T(t)$ and q can be related to the thermal conductivity λ of the fluid by:

$$\Delta T(t) = \frac{q}{4 \cdot \pi \cdot \lambda} \cdot \ln\left(\frac{4 \cdot \kappa \cdot t}{r^2 \cdot e^\gamma}\right), \tag{1}$$

where κ is the thermal diffusivity of the fluid, r is the radius of the wire, and $\gamma = 0.5772156649\ldots$ is the Euler constant.

2.2 The Measuring System

The measuring system was described in detail in our previous work [12]; here only the key information is summarized. The wires with different lengths (0.1515 m and 0.0466 m) were made from platinum (The Nilaco Corporation, JP) and had diameters of approximately 10 μm. They were spotted welded to connecting wires and mounted inside a cylindrical cavity placed within a high pressure vessel which can operate at temperatures up to 700 K and pressures up to 42 MPa. The pressure vessel was placed within a temperature controlled liquid bath. The specifications for the primary equipment used within this THW apparatus were reported together with their uncertainties by Mylona et al. [12]. The dummy resistor (R_{D}) has a resistance equal to the total resistance of the Wheatstone bridge, which allows for a more ideal step impulse when the bridge is energized.

Table 1 Gas sample information

Chemical name	CAS reg. no.	Source	Purity/mole fraction	Purification method
Methane	74-82-8	Coregas	0.99 995[a]	None
Argon	7440-37-1	Coregas	0.99 999[b]	None
Propane	74-98-6	Coregas	0.9 999[c]	None
Heptane	142-82-5	Merck	0.99[d]	None
$C_1 + C_3$ mixtures[e]	N/A	CAC Gas	0.8 999 C_1 + 0.1 001 C_3 0.8 398 C_1 + 0.1 602 C_3	None

[a]Impurities (stated by supplier): $x(H_2O) \leq 5 \times 10^{-6}$, $x(O_2) \leq 4 \times 10^{-6}$, $x(\text{other } C_mH_n) \leq 20 \times 10^{-6}$, $x(N_2) \leq 20 \times 10^{-6}$, $x(H_2) \leq 1 \times 10^{-6}$, where x denotes mole fraction

[b]Impurities (stated by supplier): $x(H_2O) \leq 1.5 \times 10^{-6}$, $x(O_2) \leq 1.0 \times 10^{-6}$, $x(C_mH_n) \leq 0.5 \times 10^{-6}$, $x(CO_2) \leq 0.5 \times 10^{-6}$, $x(N_2) \leq 5.0 \times 10^{-6}$

[c]The main impurities are the other hydrocarbons

[d]Impurities (stated by supplier): $x(H_2O) \leq 1.0 \times 10^{-4}$, $x(C_6H_6) \leq 0.1 \times 10^{-2}$, $x(S) \leq 0.5 \times 10^{-4}$, Evaporation residue $\leq 0.1 \times 10^{-4}$

[e]The $(C_1 + C_3)$ gas mixtures supplied had a certified standard relative uncertainty of 0.01 in the propane mole fraction, i.e., $u(x_{C3H8}) = 0.01 \cdot x_{C3H8}$

Table 2 Mole fraction compositions of the mixtures prepared, with expanded ($k=2$) uncertainties in the last two decimal places indicated as subscripts in brackets

Mixtures	Components/mole fraction		
	Methane	Propane	Heptane
1	$0.855_{(23)}$	$0.095_{(23)}$	$0.050_{(18)}$
2	$0.810_{(23)}$	$0.090_{(22)}$	$0.100_{(17)}$
3	$0.714_{(22)}$	$0.136_{(21)}$	$0.150_{(19)}$

2.3 Experimental Materials

The pure fluids were provided by Coregas and Merck. Methane + propane binary gas mixtures were supplied by CAC Gas. They were used as received from the supplier without further gas analysis or purification. Detailed information regarding the sample gases is listed in Table 1. As described by Al Ghafri et al. [26], the ternary mixtures (details presented in Table 2) were prepared volumetrically in our laboratory as detailed in Sect. 2.4. The expanded uncertainty ($k=2$) in composition of the mixtures was estimated to be less than 0.020 mol fraction, as detailed in Ref. [26]. This estimated composition uncertainty reflects the difficulty of preparing homogenous mixtures that are two-phase at ambient temperature. Additionally, for these ternary mixtures, particularly those with high concentrations of heptane, stratification (de-mixing) in the measurement cell was occasionally inferred when measurements made on samples stored for a long period of time without agitation exhibited increased scatter. This potential for de-mixing was included in the composition uncertainty calculations.

2.4 Experimental Procedure

Ternary mixtures used in this work were prepared following the procedure described in Al Ghafri et al. [26, 27]. In summary, the procedure consisted of transferring known volumes of heptane and $C_1 + C_3$ gas mixture (using syringe pumps) into a high pressure syringe pump that contained a mixing capability. Once all the components had been loaded, they were then mixed at high pressure (30 MPa) under liquid phase conditions for a period of 24 h or more. Before loading each mixture, the THW apparatus was flushed, evacuated, and then pressurized with pure methane to around 30 MPa which is way above the mixture's saturation pressure using a second syringe pump. The two syringe pumps were then used to inject the prepared mixture into the cell by displacing the methane at constant pressure. This displacement continued until at least three times the total volume of the cell and transfer lines had passed through the cell. Once the displacement process was completed, the mixture was left for a few hours to stabilize before measurements commenced. This procedure ensured that no phase transition inadvertently occurred during sample mixture transfer.

At each T-p state point, at least two repeat measurements were carried out; and along each isotherm, two state points with the same pressure were measured to check the repeatability. Additional thermal conductivity data were acquired along isotherms in the liquid phase near the phase boundary with pressure decreasing in steps until the mixture was approximately 1.0 MPa higher than the bubble point predicted by the GERG-2008 EOS [28]. The measured data were then linearly regressed against density (estimated using the GERG-2008 EOS [28]), and then the thermal conductivity of the saturated liquid was estimated by extrapolating the linear correlation to the predicted bubble point condition.

2.5 Uncertainty

The Guide to the Expression of Uncertainty in Measurement [29] was followed to determine the uncertainty of the thermal conductivity measurements by considering various aspects of the experiment and data analysis: the measured quantities, parameters, calculations and compositions of the mixture were considered and analyzed with the contribution for each criterion previously [12]. A budget for the combined uncertainty in the thermal conductivity $U(\lambda)$ is summarized in Table 3 with the measurement of the mixture (0.855 methane + 0.095 propane + 0.050 heptane) at $T = 200.2$ K and $p = 25.98$ MPa taken as an example condition. Note that unless otherwise stated, all uncertainties in this work are expanded uncertainties ($k = 2$) with a confidence level of 95 %. The simplification and correction of the model for $\Delta T(t)$ from measured $\Delta T_L(t)$, and the scatter of repeated measurements are the dominant contributions to the experimental uncertainty. The value $U(\lambda)/\lambda$ was estimated to be less than 0.02 for single phase pure fluid measurements, and between 0.015 and 0.056 for the single phase mixture measurements. The relative combined expanded uncertainty of the extrapolated bubble point thermal conductivity data ranges from 0.03 to 0.10.

Table 3 Uncertainty budget for the thermal conductivity. The contributions refer to the measurement of (0.855 methane + 0.095 propane + 0.050 heptane) at $T = 200.2$ K and $p = 25.98$ MPa

Source	Uncertainty U ($k=2$)	Contribution to $U(\lambda)/\lambda$ ($k=2$)
Temperature	100 mK	0.0 002
Voltage on standard resistor V_{std}	$0.0\,002 \cdot V_{std}$	0.0 002
Bridge imbalance $V_{balance}$	$0.003 \cdot V_{balance}$	0.003
Variable resistor R_2	$0.0\,005 \cdot R_2$	0.0 003
Power supply V_{power}	$0.001 \cdot V_{power}$	0.002
Wire radius (5.0 μm)	0.1 μm	0.0 001
Heat capacity of the wire c_p	$0.02 \cdot c_p$	0.0 001
The standard resistor R_{std}	$0.001 \cdot R_{std}$	0.0 011
Resistance of the long wire R_{long}	$0.001 \cdot R_{long}$	0.0 005
Resistance of the short wire R_{short}	$0.002 \cdot R_{short}$	0.0 015
Resistance of the working wire R_w	$0.003 \cdot R_w$	0.003
Length of the long wire (0.1 515 m)	0.0 002 m	0.0 019
Length of the short wire (0.0 466 m)	0.0 002 m	0.0 019
Regression	10 % of data	0.002
Simplification & correction of the ideal model Eq. 1[a]	$0.01 \cdot \lambda$	0.01
Scatter of the repeated measurements	$0.012 \cdot \lambda$	0.012
Composition	0.020 mol frac	0.022
Combined expanded uncertainty ($k=2$) for this mixture $U(\lambda)/\lambda$		0.028

Uncertainty contributions to $U(\lambda)/\lambda$ associated with pressure measurement p, parameters R_1, R_3, R_4, $R_{L,lead}$, $R_{S,lead}$, α_T, r_{cell}, ρ, c_p and $\rho_{,wire}$, are less than 0.0 001

[a]The major simplifications and corrections to the ideal model are those associated with the two-wire technique, the finite heat capacity of the wire, and the boundary confining the fluid to a finite space. See Mylona et al. [12] and Kim et al. [13] for further detail

3 Results

3.1 Validation Measurements

The apparatus was validated by means of measurements of pure methane and pure argon. The measurements were carried out at (304, 312, 324, 374 and 424) K with pressures up to 31 MPa for argon and at (312, 368 and 424) K and up to 31 MPa for methane. The experimental temperature increase of the wire ΔT as a function of time t, and the relative deviations from the fit to Eq. 1 *vs* ln(t) are shown in Fig. 2 for an argon measurement at $T = 304.2$ K and $p = 1.63$ MPa. The measured ΔT values deviate by less than 0.10 % from the linear fit to ln(t), indicating correct operation of the THW sensor for the current measurements.

The experimental (T, p, λ) data acquired for argon and methane are listed in Table 4. The relative deviations of the experimental thermal conductivities measured this work and taken from the NIST TDE database [30] for methane and argon from the values calculated using the reference equations (methane [31] and argon [32])

Fig. 2 The experimental temperature increase of the wire ΔT as a function of time t (a) and $\ln(t)$ (b), respectively, for the argon measurement at $T = 304.2$ K and $p = 1.63$ MPa. (c) Relative deviations of ΔT from the fit ΔT_{fit} to Eq. 1 vs $\ln(t)$. ○, measured points; × indicating the start and end times for the fit
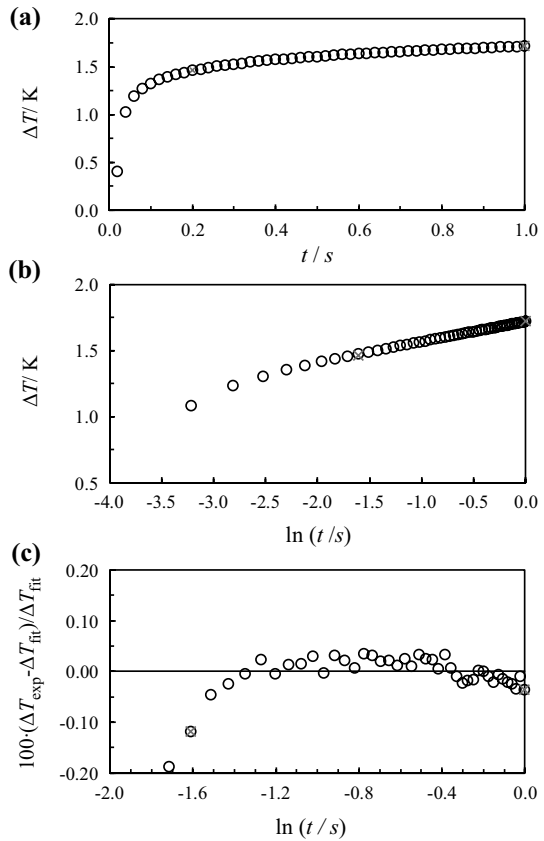
as implemented in REFPROP 10 [33] are depicted in Fig. 3. In general, the relative deviations of our experimental values from the reference equations are within the scatter of the literature data. The relative deviations are less than 2.0 % for argon and 2.5 % for methane. The reported relative uncertainties of these reference equations in the investigated temperature and pressure range are 0.02 for argon [34] and methane [35]; our measurements are generally within the uncertainty of these equations.

3.2 Mixture Measurements

Measurements of the three (methane + propane + heptane) ternary mixtures were carried out over the temperature range from (199.1 to 424.2) K and the pressure range from (10.41 to 31.55) MPa. An experimental temperature increase (ΔT) of approximately 2 K was adopted for the measurements from (228 to 424) K, while for measurements at temperatures lower than 228 K, the temperature increase ΔT was reduced to around 1 K because of convection effects that decreased the measurement accuracy. The measurement results are listed in Tables 5, 6, 7, 8, 9 and 10 and illustrated in Figs. 4, 5 and 6 for each mixture. The combined expanded uncertainty of

Table 4 The thermal conductivity of methane and argon measured in this work

T/K	p/MPa	λ/W·m^{-1}·K^{-1}	T/K	p/MPa	λ/W·m^{-1}·K^{-1}	T/K	p/MPa	λ/W·m^{-1}·K^{-1}
Methane								
423.9	30.21	0.0 763	367.5	27.43	0.0 687	312.2	25.79	0.0 683
423.6	27.34	0.0 741	367.7	25.77	0.0 666	312.3	24.18	0.0 654
423.4	25.81	0.0 729	367.9	24.14	0.0 649	312.1	20.69	0.0 607
423.5	23.97	0.0 711	367.9	20.61	0.0 619	312.2	17.27	0.0 553
423.5	20.54	0.0 686	368.1	17.15	0.0 586	313.1	13.80	0.0 502
423.4	17.24	0.0 657	368.3	13.73	0.0 553	312.6	10.32	0.0 458
423.7	13.49	0.0 623	368.3	10.34	0.0 519	312.0	4.57	0.0 390
423.7	10.22	0.0 605	368.9	4.85	0.0 478	312.3	1.70	0.0 363
367.4	31.22	0.0 724						
Argon								
424.4	12.30	0.0 269	324.6	8.19	0.0 221	312.7	10.32	0.0 229
424.7	10.18	0.0 265	324.3	6.17	0.0 211	312.8	4.91	0.0 202
424.8	8.16	0.0 258	324.3	4.16	0.0 204	304.1	12.13	0.0 235
424.8	6.17	0.0 251	324.3	2.13	0.0197	304.1	10.20	0.0 224
425.3	4.12	0.0 247	312.2	31.08	0.0 345	304.2	8.17	0.0 214
426.5	2.12	0.0 243	312.2	27.38	0.0 326	304.5	6.14	0.0 204
374.4	10.21	0.0 247	312.3	25.85	0.0 319	304.8	4.13	0.0 195
374.6	8.19	0.0 239	312.2	24.16	0.0 305	305.3	2.14	0.0 187
374.3	6.17	0.0 231	312.5	20.37	0.0 283	304.2	1.63	0.0 184
374.6	4.15	0.0 225	312.7	17.17	0.0 266	304.4	1.14	0.0 182
374.6	2.14	0.0 220	312.7	13.79	0.0 248	304.1	0.61	0.0 180

The expanded uncertainties ($k=2$) of the measurements are 0.1 K for temperature T, 0.04 MPa for pressure p, and for thermal conductivity λ, less than 0.02·λ

the thermal conductivity $U(\lambda)$ for each measurement point is listed in Tables 5, 6, 7, 8, 9 and 10 as well.

In each of the three figures, a summary of the T-p state points is shown in subfigure (a) along with the predicted phase envelopes calculated with the GERG-2008 EOS [28] as implemented in the software REFPROP 10 [33]. The experimental thermal conductivity as a function of density is illustrated in subfigures (b), and the relative deviations of the experimental thermal conductivity from values calculated with the ECS model [36] as implemented in REFPROP 10 [33] and with the SUPER-TRAPP model [37] as implemented in MultiFlash [38], respectively, are illustrated in subfigures (c). The relative deviations from the ECS model [36] are from (− 5.7 to 2.4) % and from the SUPERTRAPP model are from (− 21.1 to − 0.6) %.

The measurements used to estimate the thermal conductivity of the saturated liquid at the bubble point are illustrated in subfigure (d). The thermal conductivity values obtained at the bubble point condition were obtained by extrapolation of these data to the EOS-predicted saturation density. Considering the measurement uncertainty in the condensed phase, the uncertainty of the bubble point density

Fig. 3 Relative deviations of the experimental thermal conductivities λ_{exp} from values λ_{calc} calculated with each fluid's reference equation (methane [31] and argon [32]). Symbols: ○, data measured in this work; ×, data from the literature as obtained from the NIST TDE database [30]. (a) Methane; (b) Argon

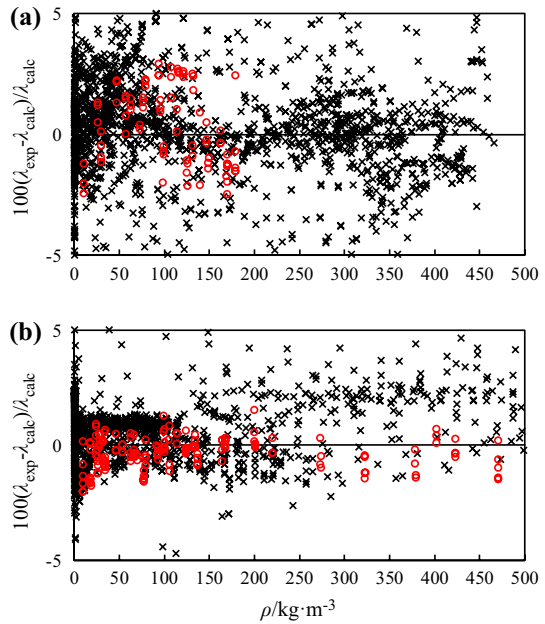**Table 5** The experimental thermal conductivity of the ternary mixture: 0.855 methane + 0.095 propane + 0.050 n-heptane

T/K	p/MPa	λ/W·m^{-1}·K^{-1}	$U(\lambda)$/W·m^{-1}·K^{-1}	T/K	p/MPa	λ/W·m^{-1}·K^{-1}	$U(\lambda)$/W·m^{-1}·K^{-1}
423.6	30.70	0.0 776	0.0 019	256.5	30.84	0.1 047	0.0 036
423.4	27.77	0.0 740	0.0 014	256.5	27.67	0.1 011	0.0 042
423.5	25.81	0.0 724	0.0 014	256.4	25.93	0.1 004	0.0 042
423.6	24.12	0.0 702	0.0 012	256.2	24.20	0.0 971	0.0 039
367.9	31.47	0.0 758	0.0 025	256.2	20.75	0.0 919	0.0 043
368.0	27.66	0.0 714	0.0 020	199.2	30.98	0.1 402	0.0 033
368.5	25.85	0.0 688	0.0 023	199.6	27.71	0.1 364	0.0 033
368.4	24.12	0.0 664	0.0 027	200.2	25.98	0.1 343	0.0 037
312.2	30.45	0.0 822	0.0 032	200.3	24.24	0.1 329	0.0 040
312.2	27.60	0.0 787	0.0 038	200.3	20.79	0.1 277	0.0 038
312.4	25.87	0.0 762	0.0 035	199.4	17.42	0.1 260	0.0 041
312.7	24.12	0.0 760	0.0 039	199.5	13.66	0.1 207	0.0 041
				199.5	10.49	0.1 161	0.0 046

The expanded uncertainties ($k=2$) of the measurements are 0.1 K for temperature T and 0.04 MPa for pressure p

calculated with GERG-2008 EOS [28], and the uncertainty due to the linear regression, the relative combined expanded uncertainty in the extrapolated bubble point thermal conductivity values was increased to between 0.03 and 0.10. This increased

Table 6 Thermal conductivity measurements for the bubble points of the ternary mixture: 0.855 methane + 0.095 propane + 0.050 n-heptane

T/K	p/MPa	λ/W·m^{-1}·K^{-1}	$U(\lambda)$/W·m^{-1}·K^{-1}	T/K	p/MPa	λ/W·m^{-1}·K^{-1}	$U(\lambda)$/W·m^{-1}·K^{-1}
229.8	19.82	0.1 037	0.0 046	203.6	10.81	0.1 143	0.0 046
229.5	17.81	0.1 001	0.0 045	206.1	8.79	0.1 087	0.0 050
229.5	15.82	0.0 971	0.0 047	206.2	6.79	0.1 043	0.0 056
229.4	14.81	0.0 957	0.0 051	205.3	5.96[a]	0.0 993	0.0 081
229.5	10.94[a]	0.0 862	0.0 071	197.7	9.61	0.1 186	0.0 045
221.1	16.56	0.1 093	0.0 045	197.9	8.52	0.1 145	0.0 047
221.3	15.53	0.1 080	0.0 048	197.7	7.80	0.1 151	0.0 048
221.3	13.51	0.1 043	0.0 048	197.6	6.79	0.1 139	0.0 052
221.2	11.50	0.1 014	0.0 054	197.5	5.80	0.1 114	0.0 051
221.2	10.51	0.0 984	0.0 054	197.4	5.29	0.1 108	0.0 052
221.2	9.23[a]	0.0 964	0.0 052	197.6	4.83[a]	0.1 005	0.0 083

The expanded uncertainties (k = 2) of the measurements are 0.1 K for temperature T and 0.04 MPa for pressure p

[a]At each bubble point, the stated pressure was estimated using the GERG-2008 EOS implemented in REFPROP 10 [33]. The thermal conductivities obtained at the bubble point condition were obtained by extrapolating the data measured near the EOS-predicted saturation density

Table 7 The experimental thermal conductivity of the ternary mixture: 0.810 methane + 0.090 propane + 0.100 n-heptane

T/K	p/MPa	λ/W·m^{-1}·K^{-1}	$U(\lambda)$/W·m^{-1}·K^{-1}	T/K	p/MPa	λ/W·m^{-1}·K^{-1}	$U(\lambda)$/W·m^{-1}·K^{-1}
423.2	31.00	0.0 766	0.0 015	256.4	31.14	0.1 117	0.0 030
423.3	27.74	0.0 736	0.0 015	256.4	27.87	0.1 083	0.0 031
423.3	26.01	0.0 721	0.0 016	256.4	26.14	0.1 080	0.0 035
423.7	24.31	0.0 697	0.0 016	256.2	24.39	0.1 051	0.0 035
367.9	31.55	0.0 774	0.0 030	256.2	20.90	0.1 007	0.0 034
367.6	27.78	0.0 728	0.0 032	200.8	31.16	0.1 432	0.0 025
367.5	25.98	0.0 718	0.0 032	200.8	27.84	0.1 412	0.0 027
367.5	24.31	0.0 699	0.0 033	200.9	26.12	0.1 404	0.0 027
311.9	30.99	0.0 908	0.0 029	200.9	24.40	0.1 394	0.0 033
311.6	27.76	0.0 873	0.0 028	200.8	20.90	0.1 344	0.0 028
311.7	26.02	0.0 852	0.0 031	200.9	17.45	0.1 311	0.0 035
311.8	24.31	0.0 833	0.0 035	200.7	13.99	0.1 296	0.0 035
				200.6	10.52	0.1 229	0.0 034

The expanded uncertainties (k = 2) of the measurements are 0.1 K for temperature T and 0.04 MPa for pressure p

Table 8 Thermal conductivity measurements for the bubble points of the ternary mixture: 0.810 methane + 0.090 propane + 0.100 n-heptane

T/K	p/MPa	λ/W·m⁻¹·K⁻¹	U(λ)/W·m⁻¹·K⁻¹	T/K	p/MPa	λ/W·m⁻¹·K⁻¹	U(λ)/W·m⁻¹·K⁻¹
300.6	27.41	0.0 904	0.0 028	230.2	20.31	0.1 080	0.0 034
300.9	25.38	0.0 873	0.0 032	230.2	18.30	0.1 049	0.0 035
300.9	23.36	0.0 856	0.0 031	230.1	16.30	0.1 022	0.0 035
300.8	22.36	0.0 840	0.0 031	230.1	14.30	0.0 993	0.0 042
300.8	20.63[a]	0.0 804	0.0 034	230.2	11.90[a]	0.0 923	0.0 090
272.9	24.30	0.0 936	0.0 033	209.3	14.29	0.1 190	0.0 035
272.9	22.31	0.0 909	0.0 034	209.3	12.27	0.1 160	0.0 035
273.0	20.34	0.0 887	0.0 034	209.1	10.25	0.1 126	0.0 040
272.9	18.26[a]	0.0 830	0.0 070	209.0	8.24	0.1 091	0.0 039
250.9	24.32	0.1 011	0.0 032	209.2	7.37[a]	0.1 042	0.0 087
250.8	22.83	0.0 994	0.0 035				
250.8	21.32	0.0 981	0.0 037				
250.7	19.29	0.0 954	0.0 039				
250.8	15.41[a]	0.0 884	0.0 087				

The expanded uncertainties (k = 2) of the measurements are 0.1 K for temperature T and 0.04 MPa for pressure p

[a]At each bubble point, the stated pressure was estimated using the GERG-2008 EOS implemented in REFPROP 10 [33]. The thermal conductivities obtained at the bubble point condition were obtained by extrapolating the data measured near the EOS-predicted saturation density

Table 9 The experimental thermal conductivity of the ternary mixture: 0.714 methane + 0.136 propane + 0.150 n-heptane

T/K	p/MPa	λ/W·m⁻¹·K⁻¹	U(λ)/W·m⁻¹·K⁻¹	T/K	p/MPa	λ/W·m⁻¹·K⁻¹	U(λ)/W·m⁻¹·K⁻¹
424.2	31.03	0.0 788	0.0 044	256.5	31.03	0.1 196	0.0 024
423.6	27.57	0.0 769	0.0 025	256.2	27.67	0.1 161	0.0 025
424.0	25.90	0.0 739	0.0 018	256.4	25.86	0.1 156	0.0 030
423.6	24.16	0.0 728	0.0 016	256.4	24.07	0.1 139	0.0 029
367.9	31.06	0.0 843	0.0 022	256.4	20.66	0.1 103	0.0 026
367.3	27.53	0.0 805	0.0 023	199.6	31.01	0.1 498	0.0 025
367.8	25.83	0.0 785	0.0 023	199.9	27.85	0.1 493	0.0 027
368.2	24.62	0.0 787	0.0 030	199.9	25.88	0.1 477	0.0 022
312.2	31.10	0.0 966	0.0 028	199.9	24.18	0.1 446	0.0 023
312.7	27.72	0.0 933	0.0 028	200.0	20.75	0.1 427	0.0 028
312.1	26.01	0.0 912	0.0 025	199.1	17.32	0.1 378	0.0 030
311.9	22.25	0.0 876	0.0 030	199.1	13.86	0.1 340	0.0 024
				199.3	10.41	0.1 303	0.0 025

The expanded uncertainties (k = 2) of the measurements are 0.1 K for temperature T and 0.04 MPa for pressure p

Table 10 Thermal conductivity measurements for the bubble points of the ternary mixture: 0.714 methane + 0.136 propane + 0.150 *n*-heptane

T/K	p/MPa	λ/W·m^{-1}·K^{-1}	$U(\lambda)$/W·m^{-1}·K^{-1}	T/K	p/MPa	λ/W·m^{-1}·K^{-1}	$U(\lambda)$/W·m^{-1}·K^{-1}
367.7	23.15	0.0 767	0.0 023	232.2	13.74	0.1 153	0.0 038
367.1	22.01	0.0 752	0.0 028	232.2	12.72	0.1 152	0.0 032
367.1	21.52	0.0 747	0.0 024	232.3	11.71	0.1 116	0.0 029
367.1	21.01	0.0 748	0.0 024	232.1	10.80[a]	0.1 121	0.0 045
367.0	20.56[a]	0.0 740	0.0 030				
320.4	22.74	0.0 854	0.0 025				
320.3	22.22	0.0 854	0.0 030				
320.2	21.80	0.0 850	0.0 026				
320.2	21.50	0.0 844	0.0 026				
320.0	19.06[a]	0.0 830	0.0 041				

The expanded uncertainties ($k=2$) of the measurements are 0.1 K for temperature T and 0.04 MPa for pressure p

[a]At each bubble point, the stated pressure was estimated using the GERG-2008 EOS implemented in REFPROP 10 [33]. The thermal conductivities obtained at the bubble point condition were obtained by extrapolating the data measured near the EOS-predicted saturation density

uncertainty was mainly due to the increased statistical uncertainty associated with the extrapolation to the bubble point condition.

3.2.1 0.855 Methane + 0.095 Propane + 0.050 Heptane

Measurements of the ternary mixture (0.855 methane + 0.095 propane + 0.050 heptane) under dense-phase conditions were carried out in the temperature range from (199.2 to 423.6) K and the pressure range from (10.49 to 31.47) MPa. The relative deviations of the data from the ECS model range between (−4 and 2) % and from the SUPERTRAPP model range from (−14 to−1) %. Four thermal conductivity values at bubble points of (229.5 K, 10.94 MPa), (221.2 K, 9.23 MPa), (205.3 K, 5.96 MPa) and (197.6 K, 4.83 MPa) were estimated by means of extrapolation. The relative deviations of these extrapolated estimates from values calculated with the ECS model range from (4 to 8) %.

3.2.2 0.810 Methane + 0.090 Propane + 0.100 Heptane

Measurements of the ternary mixture (0.810 methane + 0.090 propane + 0.100 heptane) under dense-phase conditions were carried out in the temperature range from (200.6 to 423.7) K and the pressure range from (10.52 to 31.55) MPa. The relative deviations of the data from the ECS model range between (−6 and 0) % and from the SUPERTRAPP model range from (−21 to−3) %. Five thermal conductivities at bubble points of (300.8 K, 20.63 MPa), (272.9 K, 18.26 MPa), (250.8 K, 15.41 MPa), (230.2 K, 11.90 MPa) and (209.2 K, 7.37 MPa) were estimated by means of extrapolation. The relative deviations of these extrapolated estimates from values calculated with the ECS model range from (3 to 10) %.
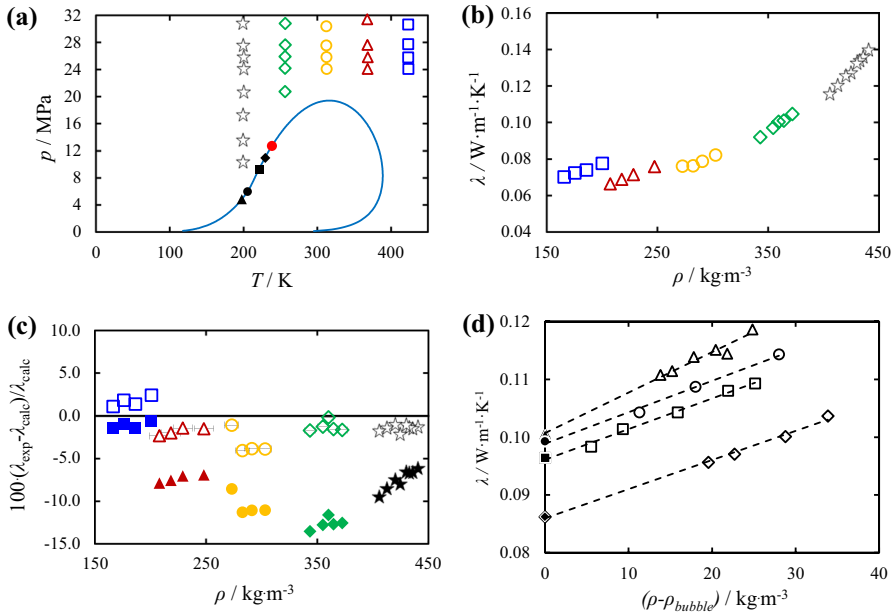
Fig. 4 Thermal conductivity measurements of the ternary mixture (0.855 methane + 0.095 propane + 0.050 heptane). Symbols for (a–c) ($\star$, $T = 199$ K; ($\diamond$ $\blacklozenge$, $T = 256$ K; ($\circ$ $\bullet$, $T = 312$ K; ($\triangle$ $\blacktriangle$, $T = 368$ K; ($\square$ $\blacksquare$, $T = 423$ K). (a) The pressure–temperature phase diagram and the measurement conditions investigated; the phase boundaries (blue solid curves) together with bubble points (filled symbols) were calculated with GERG-2008 EOS [28] and the critical points ($\bullet$) was obtained from REFPROP 10 [33]. (b) The experimental thermal conductivity λ_{exp} as a function of fluid density ρ. (c) The relative deviations of the experimental thermal conductivity λ_{exp} from values λ_{calc} calculated with the ECS model [36] as implemented in REFPROP 10 [33] (empty symbols) and with the SUPERTRAPP model [37] as implemented in MultiFlash [38] (filled symbols). (d) Experimental thermal conductivity as a function of $\Delta\rho = (\rho - \rho_{bubble})$, where ρ_{bubble} is the density at the bubble point as estimated by the GERG-2008 EOS. Symbols: ($\triangle$, $T = 198$ K; $\circ$, $T = 205$ K; $\square$, $T = 221$ K; $\diamond$, $T = 230$ K). The straight lines were regressed to the measured (hollow) data points and extrapolated to estimate the thermal conductivity (filled symbols) at the bubble point (color figure online)

3.2.3 0.714 Methane + 0.136 Propane + 0.150 Heptane

Measurements of the ternary mixture (0.714 methane + 0.136 propane + 0.150 heptane) under dense-phase conditions were carried out in the temperature range from (199.1 to 424.2) K and the pressure range from (10.41 to 31.10) MPa. The relative deviations of the data from the ECS model range between (-4 and -1) % and from the SUPERTRAPP model range from (-20 to -4) %. Three thermal conductivities at bubble points of (367.0 K, 20.56 MPa), (320.0 K, 21.06 MPa) and (232.1 K, 10.80 MPa) were estimated by means of extrapolation. The relative deviations of these extrapolated estimates from values calculated with the ECS model range from (3 to 5) %.
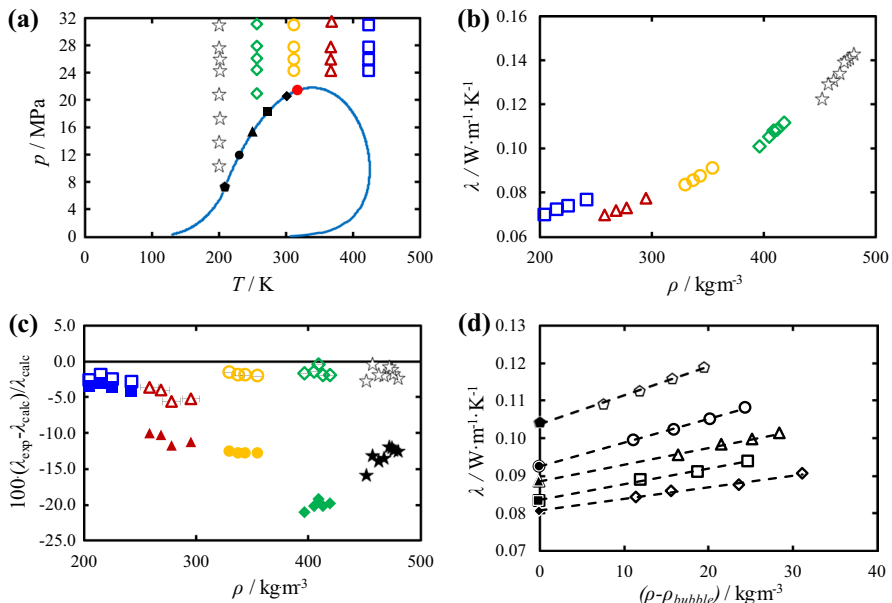
Fig. 5 Thermal conductivity measurements of the ternary mixture (0.810 methane + 0.090 propane + 0.100 heptane). Symbols for (a–c) (☆ ★, $T = 199$ K; ◇ ◆, $T = 256$ K; ○ ●, $T = 312$ K; △ ▲, $T = 368$ K; □ ■, $T = 423$ K). (a) The pressure–temperature phase diagram and the measurement conditions investigated; the phase boundaries (blue solid curves) together with bubble points (filled symbols) were calculated with GERG-2008 EOS [28] and the critical points (●) was obtained from REFPROP 10 [33]. (b) The experimental thermal conductivity λ_{exp} as a function of density ρ. (c) The relative deviations of the experimental thermal conductivity λ_{exp} from values λ_{calc} calculated with the ECS model [36] as implemented in REFPROP 10 [33] (empty symbols) and with the SUPERTRAPP model [37] as implemented in MultiFlash [38] (filled symbols). (d) Experimental thermal conductivity as a function of $\Delta\rho = (\rho - \rho_{bubble})$, where ρ_{bubble} is the density point as estimated by the GERG-2008 EOS. Symbols: (⬠, $T = 209$ K; ○, $T = 230$ K; △, $T = 251$ K; □, $T = 273$ K; ◇, $T = 300$ K). The straight lines were regressed to the measured (hollow) data points and extrapolated to estimate the thermal conductivity (filled symbols) at the bubble point (color figure online)

4 Conclusions

Natural gas processing applications have an increasing need for reliable data and property predictions at conditions near the phase boundary and the critical point. For this purpose, thermal conductivity measurements of three different ternary mixtures containing (methane + propane + heptane) were carried out in the temperature range from (199.1 to 424.2) K and the pressure range between (10.41 and 31.55) MPa. The thermal conductivity measurements were performed with an apparatus using the transient hot-wire technique, with relative combined expanded uncertainties ($k = 2$) under dense-phase conditions ranging from 0.015 to 0.056.

The experimental data were compared to values calculated by the extended corresponding states (ECS) model and SUPERTRAPP model implemented in the software packages REFPROP 10 and MultiFlash 6.2, respectively. The dense-phase data
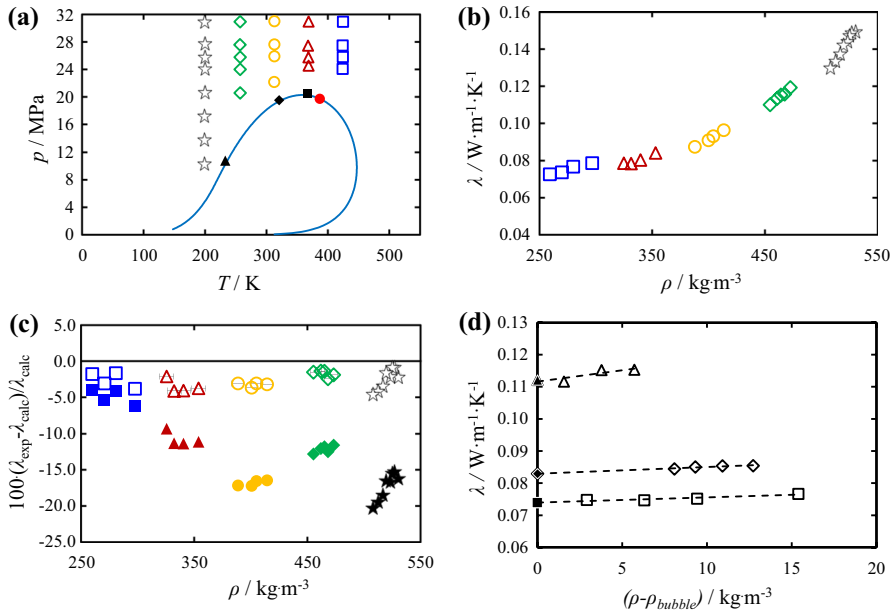
Fig. 6 Thermal conductivity measurements of the ternary mixture (0.714 methane + 0.136 propane + 0.150 heptane). Symbols for (a–c) (☆ ★, $T = 199$ K; ◇ ◆, $T = 256$ K; ○ ●, $T = 312$ K; △ ▲, $T = 368$ K; □ ■, $T = 423$ K). (a) The pressure–temperature phase diagram and the measurement conditions investigated; the phase boundaries (blue solid curves) together with bubble points (filled symbols) were calculated with GERG-2008 EOS [28] and the critical points (●) was obtained from REFPROP 10 [33]. (b) The experimental thermal conductivity λ_{exp} as a function of density ρ. (c) The relative deviations of the experimental thermal conductivity λ_{exp} from values λ_{calc} calculated with the ECS model [36] as implemented in REFPROP 10 [33] (empty symbols) and with the SUPERTRAPP model [37] as implemented in MultiFlash [38] (filled symbols). (d) Experimental thermal conductivity as a function of $\Delta\rho = (\rho - \rho_{bubble})$, where ρ_{bubble} is the density at the bubble point as estimated by the GERG-2008 EOS. Symbols: $(\triangle, T = 232$ K; $\diamond$, $T = 320$ K; $\square$, $T = 367$ K$)$. The straight lines were regressed to the measured (hollow) data points and extrapolated to estimate the thermal conductivity (filled symbols) at the bubble point (color figure online)

had relative deviations from the ECS model predictions ranging between $(-5.7$ and $2.4)$ %, which is comparable with the experimental uncertainty of the data. Accordingly, further tuning of binary interaction parameters within the ECS model does not appear warranted. In contrast the data systematically deviate from the SUPERTRAPP model predictions by between $(-21.1$ and $-0.6)$ %. This work clearly demonstrates the value of experimental data for testing the predictive models used to design and optimize natural gas processing systems, and identifies the ECS model as the most suitable for calculations involving high pressure natural gas mixtures.

References

1. A. Arami-Niya, X. Xiao, S. Al Ghafri, F. Jiao, M. Khamphasith, E.S. Pouya, M. Seyyedsadaghiani, X. Yang, T. Tsuji, Y. Tanaka, Y. Seiki, E.F. May, Int. J. Refrig. (2020). https://doi.org/10.1016/j.ijrefrig.2020.05.009
2. S.Z.S. Al Ghafri, T.J. Hughes, F. Perez, C.J. Baker, A. Siahvashi, A. Karimi, A. Arami-Niya, E.F. May, Fluid Phase Equilib. **518**, 112620 (2020). https://doi.org/10.1016/j.fluid.2020.112620
3. S.Z.S. Al Ghafri, J.P.M. Trusler, J. Supercrit. Fluids **145**, 1 (2019). https://doi.org/10.1016/j.supflu.2018.11.012
4. M. Akhfash, S.Z.S. Al Ghafri, D. Rowland, T.J. Hughes, T. Tsuji, Y. Tanaka, Y. Seiki, E.F. May, J. Chem. Eng. Data (2019). https://doi.org/10.1021/acs.jced.8b01039
5. L.F.S. Souza, S.Z.S. Al Ghafri, J.P.M. Trusler, J. Chem. Thermodyn. **126**, 63 (2018). https://doi.org/10.1016/j.jct.2018.06.022
6. Y. Sanchez-Vicente, W.J. Tay, S.Z. Al Ghafri, J.P.M. Trusler, Appl. Energy **220**, 629 (2018). https://doi.org/10.1016/j.apenergy.2018.03.136
7. F.F. Czubinski, S.Z.S. Al Ghafri, T.J. Hughes, P.L. Stanwix, E.F. May, Fuel **225**, 563 (2018). https://doi.org/10.1016/j.fuel.2018.03.183
8. S.Z.S. Al Ghafri, F.F. Czubinski, E.F. May, Fuel **231**, 187 (2018). https://doi.org/10.1016/j.fuel.2018.05.087
9. A. Siahvashi, S.Z.S. Al Ghafri, J.H. Oakley, T.J. Hughes, B.F. Graham, E.F. May, J. Chem. Eng. Data **62**, 2896 (2017). https://doi.org/10.1021/acs.jced.7b00171
10. S.Z.S. Al Ghafri, G.C. Maitland, J.P.M. Trusler, J. Chem. Eng. Data **62**, 2826 (2017). https://doi.org/10.1021/acs.jced.7b00145
11. S.K. Mylona, T.J. Hughes, A.A. Saeed, D. Rowland, J. Park, T. Tsuji, Y. Tanaka, Y. Seiki, E.F. May, J. Chem. Thermodyn. **133**, 135 (2019). https://doi.org/10.1016/j.jct.2019.01.028
12. S.K. Mylona, X. Yang, T.J. Hughes, A.C. White, L. McElroy, D. Kim, S. Al Ghafri, P.L. Stanwix, Y.H. Sohn, Y. Seo, E.F. May, J. Chem. Eng. Data **65**, 906 (2020). https://doi.org/10.1021/acs.jced.9b01087
13. D. Kim, X. Yang, A. Arami-Niya, D. Rowland, X. Xiao, S. Al Ghafri, T. Tsuji, Y. Tanaka, Y. Seiki, E.F. May, J. Chem. Thermodyn. **151**, 106248 (2020)
14. R.A. Perkins, M.L. Huber, M.J. Assael, J. Chem. Eng. Data **61**, 3286 (2016)
15. R.A. Perkins, M.L. Huber, M.J. Assael, J. Chem. Eng. Data **62**, 2659 (2017)
16. G.J. Tertsinidou, C.M. Tsolakidou, M. Pantzali, M.J. Assael, L. Colla, L. Fedele, S. Bobbo, W.A. Wakeham, J. Chem. Eng. Data **62**, 491 (2016)
17. K.D. Antoniadis, G.J. Tertsinidou, M.J. Assael, W.A. Wakeham, Int. J. Thermophys. **37**, 78 (2016). https://doi.org/10.1007/s10765-016-2083-8
18. X. Wang, S. Qiu, J. Wu, I.M. Abdulagatov, J. Chem. Eng. Data **65**, 1993 (2020)
19. X. Li, J. Wu, Q. Dang, J. Chem. Eng. Data **55**, 1241 (2010)
20. W.A. Wakeham, A. Nagashima (eds.), *Experimental Thermodynamics. Vol. III, Measurement of the Transport Properties of Fluids* (Blackwell Scientific Publications, London, 1991)
21. M.J. Assael, K.D. Antoniadis, W.A. Wakeham, Int. J. Thermophys. **31**, 1051 (2010). https://doi.org/10.1007/s10765-010-0814-9
22. R.A. Perkins, H.M. Roder, C.A. Nieto de Castro, J. Res. Natl. Inst. Stand. Technol. **96**, 247 (1991)
23. K.N. Marsh, R.A. Perkins, M.L. Ramires, J. Chem. Eng. Data **47**, 932 (2002)
24. J. Kestin, W.A. Wakeham, Phys. A **92**, 102 (1978)
25. J.J. Healy, J.J. de Groot, J. Kestin, Physica B+C **82**, 392 (1976)
26. S.Z. Al Ghafri, F. Jiao, T.J. Hughes, A. Arami-Niya, X. Yang, A. Siahvashi, A. Karimi, E.F. May, Fuel **304**, 121395 (2021)
27. S.Z. Al Ghafri, D. Rowland, M. Akhfash, A. Arami-Niya, M. Khamphasith, X. Xiao, T. Tsuji, Y. Tanaka, Y. Seiki, E.F. May, Int. J. Refriger. **98**, 249 (2019)
28. O. Kunz, W. Wagner, J. Chem. Eng. Data **57**, 3032 (2012)
29. ISO/IEC Guide 98: Uncertainty of measurement—part 3: Guide to the expression of uncertainty in measurement (GUM: 1995) (2008)
30. M. Frenkel, R.D. Chirico, V. Diky, X. Yan, Q. Dong, C. Muzny, J. Chem. Inf. Model. **45**, 816 (2005)
31. D.G. Friend, J.F. Ely, H. Ingham, J. Phys. Chem. Ref. Data **18**, 583 (1989)
32. E.W. Lemmon, R.T. Jacobsen, Int. J. Thermophys. **25**, 21 (2004)
33. E.W. Lemmon, I.H. Bell, M.L. Huber, M.O. McLinden. (2018). http://www.nist.gov/srd/nist23.cfm.

34. C. Tegeler, R. Span, W. Wagner, J. Phys. Chem. Ref. Data **28**, 779 (1999)
35. U. Setzmann, W. Wagner, J. Phys. Chem. Ref. Data **20**, 1061 (1991)
36. J.C. Chichester, M.L. Huber, *Documentation and assessment of the transport property model for mixtures implemented in NIST REFPROP (Version 8.0)*. National Institute of Standards and Technology (2008)
37. M.L. Huber, H.J.M. Hanley, *Transport Prop. The Corresponding-States Principle: Dense fluids*, ed. by J. Millat, J.H. Dymond, C.A. Nieto de Castro. Transport Properties of Fluids: Their Correlation, Prediction and Estimation, vol 285 (Cambridge University Press, New York, 1996), pp. 283–295
38. KBC InfoChem, *Advanced Technologies PLC Multiflash*, vol. 6 (KBC InfoChem, Doha, 2019)

Publisher's Note Springer Nature remains neutral with regard to jurisdictional claims in published maps and institutional affiliations.